

Frustrated Altermagnetism and Charge Density Wave in Kagome Superconductor CsCr_3Sb_5

Chenchao Xu,^{1,2} Siqi Wu,³ Guo-Xiang Zhi,⁴ Guanghan Cao,³
 Jianhui Dai,¹ Chao Cao,^{3,2,*} Xiaoqun Wang,^{3,†} and Hai-Qing Lin^{3,‡}

¹*School of Physics, Hangzhou Normal University, Hangzhou 310036, P. R. China*

²*Center for Correlated Matter, Zhejiang University, Hangzhou 310058, China*

³*School of Physics, Zhejiang University, Hangzhou 310058, China*

⁴*Tianmushan Laboratory, Hangzhou 310023, China*

(Dated: September 27, 2023)

Using first-principles density-functional calculations, we investigate the electronic structure and magnetism of the kagome superconductor CsCr_3Sb_5 . At the ambient pressure, its ground state is found to be 4×2 altermagnetic spin-density-wave (SDW) pattern, with an averaged effective moment of $\sim 1.7\mu_B$ per chromium atom. The magnetic long range order is coupled to the lattice structure, generating $4a_0$ structural modulation. However, multiple competing SDW phases are present and energetically very close, suggesting strong magnetic fluctuation and frustration. The electronic states near the Fermi level are dominated by Cr-3d orbitals, and flat band or van Hove singularities are away from the Fermi level. When external pressure is applied, the energy differences between competing orders and the structural modulations are suppressed by external pressure. The magnetic fluctuation remains present and important at high pressure because the non-magnetic phase is unstable up to 30 GPa. In addition, a bonding state between Cr-3d_{xz} and Sb^{II}-p_z quickly acquires dispersion and eventually becomes metallic around 5 GPa, leading to a Lifshitz transition. Our findings strongly support unconventional superconductivity in the CsCr_3Sb_5 compound above 5 GPa, and suggest crucial role of magnetic fluctuations in the pairing mechanism.

Kagome lattice has been one of the most intriguing systems[1] since its original proposal[2] in 1951. As one of the most frustrated geometry, the ground state of spin-1/2 kagome lattice is widely believed to be quantum spin liquid (QSL), but its nature is still under hot debate[3–9]. Once slightly doped, a superconducting phase may emerge from the proposed $U(1)$ Dirac QSL[10]. For spin-1 kagome lattices, model studies point to trimerized or simplex valence bond solid as its ground state[11–13]. Beyond the spin models, the electronic and phonon band structure of kagome lattice exhibits topological flat bands due to the destructive interference between Bloch waves[14, 15], in addition to the Dirac cones and van Hove singularities. Notably, nontrivial physical properties including kinetic ferromagnetism[16], fractional Quantum Hall effect[14] and large band-specific diamagnetism[17] may emerge from the flat bands. Moreover, near the van Hove fillings, different orders include charge density wave (CDW), chiral spin density wave (cSDW), chiral d -wave superconductivity or even f -wave triplet superconductivity are proposed[18–21].

Of the many kagome materials, the ternary AV_3Sb_5 family has drawn much attention since its discovery[22]. Their much debated CDW order[23–30] is widely believed to be associated with the nesting between van Hove singularities[31, 32], and may breaks time-reversal symmetry and chiral[33–37]. The superconductivity was proposed to be unconventional[30, 38, 39], but evidence for conventional BCS superconductivity are also presented[40–44]. Under pressure, the CDW is suppressed and the superconductivity exhibits two-dome

structure[45, 46]. Nevertheless, despite of its rich physics and phenomena, the AV_3Sb_5 family is widely accepted that AV_3Sb_5 family is weakly correlated without local moment[40, 47].

Recently, a chromium-based kagome compound CsCr_3Sb_5 was reported to be superconducting with $T_c = 6.4$ K at pressure $p > p_c = 4$ GPa[48]. At the room temperature and ambient pressure, the CsCr_3Sb_5 compound crystallizes in hexagonal structure with space group P6/mmm (No. 191), similar to the AV_3Sb_5 family. The Cr atoms are arranged into corner-sharing triangles, forming the kagome lattice (FIG. 1). Distinguished from the AV_3Sb_5 family, the ground state of CsCr_3Sb_5 appears to be antiferromagnetic (AFM) with 4×1 CDW superstructure at ambient pressure. External pressure quickly suppresses the long range magnetic order as well as the CDW modulation at around 4GPa, where superconductivity abruptly appears with highest $T_c^{\text{max}} = 6.4$ K at $p_m = 4.2$ GPa. Beyond p_{max} , the T_c decreases, forming a dome-like structure. The upper critical field H_{c2} is well beyond the Pauli limit around the T_c^{max} , suggesting unconventional pairing mechanism. Several imminent questions are therefore needs to be addressed: 1) What is the long range order ground state? 2) What is the nature of the ordered magnetism? In particular, is the long range order local moment or itinerant? 3) How does the electronic structure evolve under pressure?

In this *Letter*, we perform systematic study on CsCr_3Sb_5 using first-principles simulations, focusing on its ground state at ambient pressure and the effect of external pressure on the electronic structure. Unlike

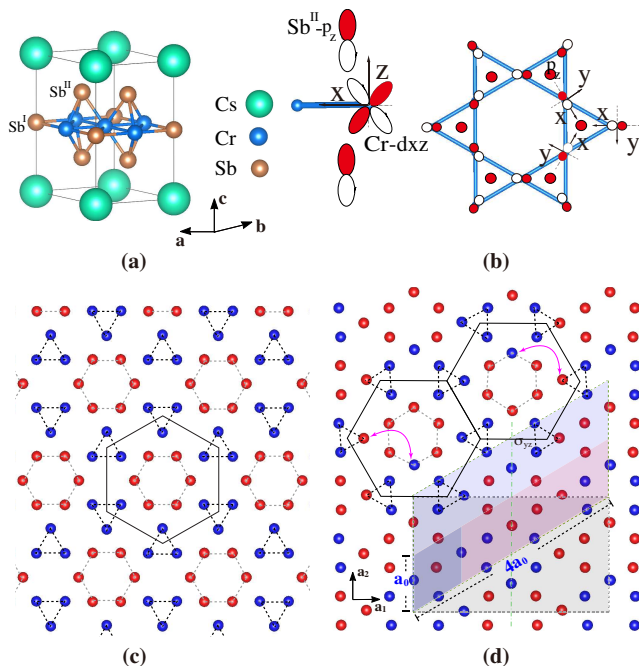


FIG. 1. (a) Crystal structure of CsCr_3Sb_5 with $P6/mmm$ symmetry. (b) Definition of local axis for Cr atoms. The local x -axis points to the center of triangles, whereas the local y -axis points to the center of hexagon. (c) AF-ISOD SDW pattern inspired by inverse star-of-david charge order. The black solid hexagon indicates its Wigner-Seitz (WS) unit cell. (d) Ground state SDW pattern (failed AF-ISOD) of CsCr_3Sb_5 at ambient pressure. The grey solid hexagons and pink arrows indicate the original WS unit cells and the swapped moments compared to the AF-ISOD pattern. The green dash-point line indicate the gliding-mirror plane. The blue shaded area shows the 4×2 supercell, whereas the red shaded area indicates the standard unit cell.

AV_3Sb_5 , the magnetic fluctuation is crucial to stabilize the lattice structure even at high pressures. The ground state at ambient pressure is a collinear 4×2 altermagnetic spin-density-wave (SDW) order. In addition, multiple SDW orders are energetically close to each other, suggesting strong fluctuation and frustration. Under pressure, the magnetic fluctuation enhances, and a Lifshitz transition due to metallization of bonding state is observed at the critical pressure p_c .

At ambient pressure, the fully optimized structure using nonmagnetic (NM) DFT calculations yields lattice constant a and all bond lengths smaller than experimental value (refer to SI for detail). This is in sharp contrast to the AV_3Sb_5 whose lattice constants and bond lengths are slightly overestimated in NM DFT calculations due to the underestimate of bonding in PBE. Such phenomenon, however, is frequently observed in compounds where magnetic fluctuations are important, including iron-pnictides/chalcogenides[49–51] and other chromium based superconductors[52, 53]. In addition, the NM phonon spectrum of CsCr_3Sb_5 at ambient pres-

sure exhibits enormous imaginary frequencies at almost every \mathbf{q} -points along the high symmetry lines, except along Γ -A (FIG. 2a), suggesting the lattice is highly unstable if the system is purely nonmagnetic.

In order to figure out the magnetic ground state for CsCr_3Sb_5 at ambient pressure, we first sort out several candidates proposed in previous model studies of spin-1/2 and spin-1 kagome lattices. In particular, collinear patterns including FM, up-up-down (UUD), inter-layer AFM (IAF), as well as noncollinear patterns including 1×1 120° -AFM, $\sqrt{3} \times \sqrt{3}$ in-plane AFM I/II, 2×2 cuboctahedron (*cuboc*) phases are considered. Inspired by the SOD/ISOD orders, we have also considered $3 \times 2 \times 2$ patterns, dubbed as AF-ISOD (FIG. 1c), in-out SOD and all-in (or all-out) SOD patterns (refer to SI). Surprisingly, the collinear orders prevail the noncollinear orders at the same magnetic cell size. In addition, patterns with net moment are energetically less favorable, indicating overall AFM tendency. Therefore, we performed a complete search of all possible collinear AFM orders up to 8 primitive cells with 24 magnetic sites. To do this, we first generate all symmetrically inequivalent configurations with 0 net moment, and then eliminate configurations have no symmetry connecting the two sublattices. This procedure yields $3 \times 2 \times 1$, $5 \times 2 \times 2$, $15 \times 4 \times 1$, $760 \times 8 \times 1$ and $1128 \times 4 \times 2$ configurations. Employing a systematic high-throughput algorithm (refer to SI for detail), we search for the magnetic ground state for CsCr_3Sb_5 . Overall, the lattice constants and bond lengths of fully relaxed structures in most magnetic cases are closer to experimental observations. The magnetic moment is quite robust around $1.8 \mu_B$ for each Cr atom in all calculations even without explicitly considering the on-site Coulomb interactions, except for the in-plane FM cases ($1.5 \mu_B/\text{Cr}$).

The magnetic ground state configuration turns out to be a complex pattern (FIG. 1d), which can be viewed as "failed AF-ISOD". For the AF-ISOD state, all Cr atoms are coordinated with exactly 2 nearest antiparallel Cr atoms, such that one can arrange nearest neighboring AF bonds to form SOD (or the nearest neighboring FM bonds to form ISOD) pattern. However, it is apparent that the spin-up sublattice is inequivalent to the spin-down sublattice in the AF-ISOD pattern, therefore it does not appear in the high-throughput 2×2 configurations. To lower the total energy, the magnetic moment of two pairs of next nearest neighboring atoms inside one unit cell are swapped, so that the two sublattices become equivalent, resulting in the failed AF-ISOD ground state pattern. The swapped atoms are uniformly distributed across all ISOD structures, and are aligned in parallel to minimize the total energy. The the in-plane alignment of moments is energetically slightly favored than out-of-plane alignment by $\sim 0.6 \text{ meV}/\text{Cr}$, supporting the experimental observation from susceptibility measurement[48]. The staggered moment ranges from 1.4 to $1.8 \mu_B$ for each Cr atoms. More importantly, it is evident that

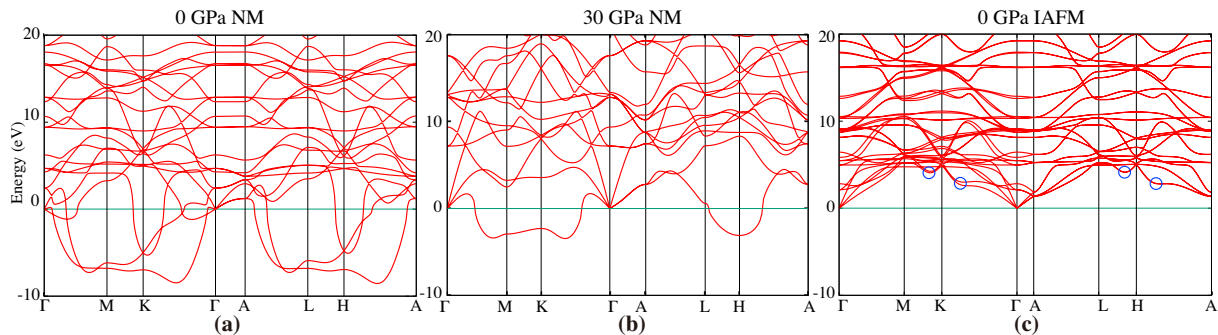


FIG. 2. (a-b) The phonon spectrum of CsCr_3Sb_5 in NM state at (a) ambient pressure and (b) 30 GPa. (c) The phonon spectrum of CsCr_3Sb_5 in IAFM state at ambient pressure. The soft modes are marked with blue circles.

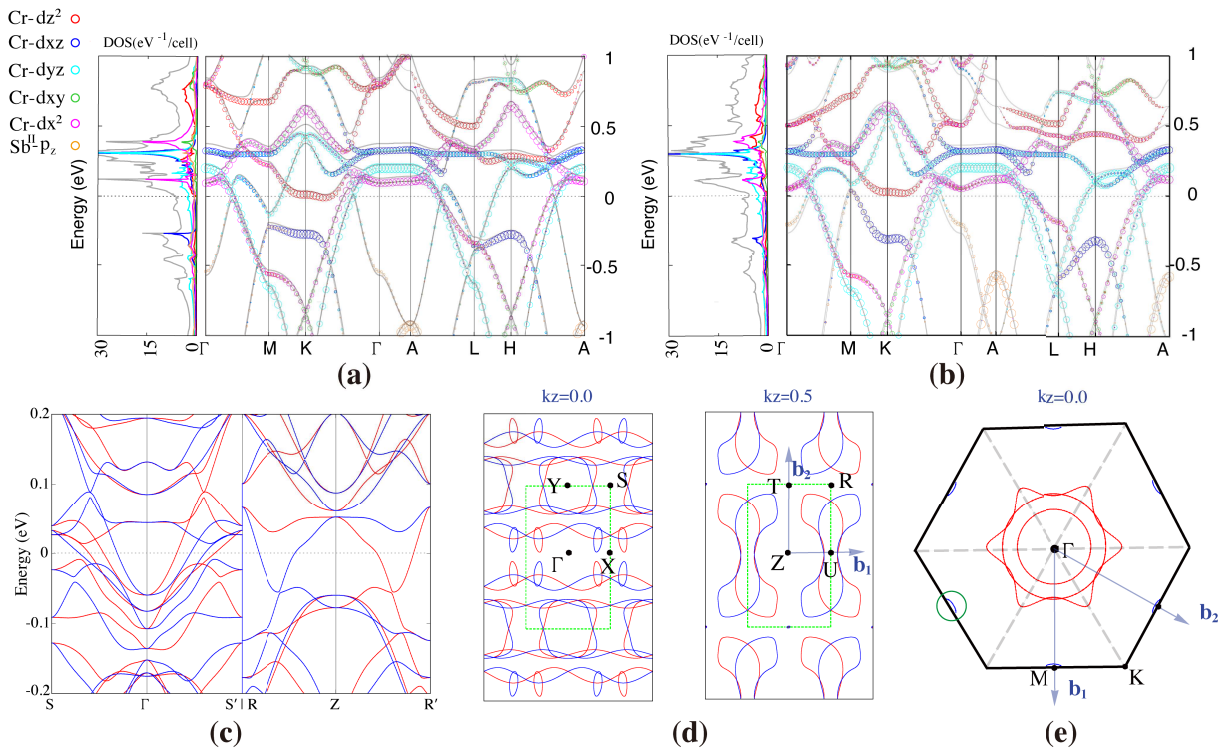


FIG. 3. (a-b) Band structure and density of states (DOS) of CsCr_3Sb_5 in the PM state at ambient pressure and 5 GPa. The size of circles are proportional to the weight of corresponding atomic orbitals. The Cr-3d orbitals are defined on local axis in FIG. 1b. (c) Band structure of CsCr_3Sb_5 in the failed AF-ISOD ground state at ambient pressure. (d) Intersection of failed AF-ISOD ground state Fermi surfaces at $k_z = 0$ and $k_z = \pi$. For (c) and (d), the red/blue lines correspond to spin-up/down, respectively; and the high symmetry points are chosen according to the standardized unit cell. (e) The intersection of PM Fermi surfaces at $k_z = 0$ plane at 5 GPa. The additional Fermi surface pocket around M due to the Lifshitz transition is indicated by green circle.

the two spin-sublattices are not connected by either simple translation or inversion. Instead, they are connected by $[\mathcal{T}|\{\sigma_{yz}|(0, 1/2, 0)\}]$, a gliding-mirror combined with time-reversal operation. Thus, the ground state at the ambient pressure is altermagnetic[54].

The formation of magnetic long range order has non-trivial effect on the lattice structure by introducing structural modulations. In our calculations, all lowest energy configurations breaks the 3-fold rotational symmetry, and

both the Cr and the Sb^{II} positions are strongly modulated. In particular, the failed AF-ISOD ground state is formed by $2 \times 4 \times 1$ stripes connected by time-reversal gliding-mirror symmetry. In addition, the leading competing order naturally consists of $2 \times 4 \times 1$ stripe order connected by time-reversal operation combined translation only, in consistent with experimentally observed 4×1 charge order at low temperature. Given these orders are energetically and both are closely resembles AF-ISOD or-

TABLE I. Total energies (in meV/Cr) with respect to NM state and magnetic moment m_{Cr} (in μ_B) of typical magnetic configurations. For AF-ISOD state, the numbers in (outside) the parenthesis are the moments of Cr on the hexagons (triangles). The magnetic patterns can be found in SI. The line in bold font is the failed AF-ISOD ground state.

Size	Pattern	0 GPa		5 GPa	
		E_{tot}	m_{Cr}	E_{tot}	m_{Cr}
$1 \times 1 \times 1$	FM	-65.0	1.5	-60.0	1.4
	UUD	-98.7	1.5	-71.8	1.3
	$\mathbf{q}=0$ NCL	-80.7	1.9	to NM	
$1 \times 1 \times 2$	IAFM	-64.6	1.5	-59.5	1.4
$\sqrt{3} \times \sqrt{3} \times 1$	NCL-1	-96.7	1.8	-74.9	1.6
	NCL-2	-81.3	1.8	-55.0	1.6
$2 \times 2 \times 1$	NCL-3	-97.1	1.8	-74.4	1.6
	NCL-4	-74.0	1.8	-55.5	1.6
	cuboc	converge to 821			
	AF-ISOD	-110.8	1.9 (1.7)	-90.0	1.8 (1.5)
$4 \times 1 \times 1$	821	-125.7	1.7	-104.5	1.6
	915	-127.1	1.8	-97.3	1.6
$4 \times 2 \times 1$	6692437	-134.5	1.7	-109.9	1.6
	6707797	-131.5	1.7	-106.6	1.6
	1550757	-121.0	1.7	-104.8	1.6
	5917545	-118.1	1.8	-98.8	1.6
	NCL-5	converge to 5917545			
$8 \times 1 \times 1$	2987565	-129.0	1.7	-101.9	1.6

ders, therefore the CDW order forms before the SDW, in consistency with the experimental observation. The formation of magnetic long range order stabilizes the lattice structure. The calculated phonon spectrum of the simplest collinear AFM state ($1 \times 1 \times 2$ IAFM) is free of the structural instability (FIG. 2c), although it is still energetically much higher than the ground state and multiple soft phonon mode can be identified.

We illustrate the electronic structure of CsCr_3Sb_5 at the ambient pressure in FIG. 3. For undistorted NM CsCr_3Sb_5 , each Cr atom is surrounded by 4 Sb^{II} atoms located directly above/below the center of kagome triangles, as well as 2 Sb^{I} atoms located at the center of kagome hexagons. These 6 nearest neighboring Sb atoms form a squashed octahedron. We take the direction pointing towards the center of kagome hexagon as the local- x axis. Most of the electronic bands were dominated by the Cr-3d orbitals, except for one dispersive band from p_z orbitals of Sb^{II} and hybridizes with d_{yz}/d_{xz} orbitals along Γ -M and Γ -K. Flat band formed by d_{xz}/d_{yz} orbitals can be identified around 300 meV above the Fermi level. Other kagome band characteristics, including the van Hove singularities (vHS) and Dirac cones can still be identified from the large-scale plots, but they are mostly far from the Fermi level. Interestingly, additional vHS can also be identified around K, most prominently around 270 meV below E_F . Along K-M, this band exhibits rather flat dispersion, giving rise to the unambiguous vHS shown in the DOS in left panel of Figure 3a. Density of state and symmetry analysis sug-

gest it a bonding state between Cr and Sb^{II} atoms. There is one another nearly flat segment of d_{z^2} orbital can also be identified around K, but no vHS can be identified from DOS. In addition, the bands are also very flat along Γ -A, suggesting quasi-two-dimensionality of its electronic structure.

For CsCr_3Sb_5 in the failed AF-ISOD ground state, the spin-degeneracy is generally lifted due to the lack of inversion or simple translation symmetry between sublattices (FIG. 1d). The spin splitting is evident along Γ -S, with largest splitting ~ 80 meV close to the Fermi level. Such splitting suggests separated spin-up/spin-down Fermi surface sheets, as evidenced in FIG. 3c. Such exotic magnetic ground state is topological, and intrinsic anomalous Hall effect is expected at the ground state[54]. Should the superconductivity is related with this magnetic ground state, spin-triplet is also enabled due to the broken inversion symmetry as a result of the spin configuration.

One would expect the energetics of the magnetic states is described by the Heisenberg spin model, which is the simplest case involves the bilinear exchange interactions as follows:

$$E = E_0 + J_1 \sum_{\langle ij \rangle} \mathbf{S}_i \cdot \mathbf{S}_j + J_2 \sum_{\langle\langle ij \rangle\rangle} \mathbf{S}_i \cdot \mathbf{S}_j + J_3 \sum_{\langle\langle\langle ij \rangle\rangle\rangle_b} \mathbf{S}_i \cdot \mathbf{S}_j + J_3^h \sum_{\langle\langle\langle ij \rangle\rangle\rangle_h} \mathbf{S}_i \cdot \mathbf{S}_j$$

Here, J_1 and J_2 are the exchange couplings between the nearest and next-nearest neighbor (denoted by $\langle \rangle$ and $\langle\langle \rangle\rangle$) Cr atoms; J_3 and J_3^h are the exchange couplings between the next-next-nearest neighbor Cr atoms along bond and across kagome hexagon (denoted by $\langle\langle\langle \rangle\rangle\rangle_b$ and $\langle\langle\langle \rangle\rangle\rangle_h$), respectively. However, the DFT total energies of all the 2×2 and 4×1 collinear configurations are failed to be fitted by these interaction parameters in a wide range distribution of the staggered Cr-moment. This suggests the necessity of including other spin-spin interactions, such as the quadratic spin-spin interactions. On the other hand, our result may also hint the important role played by the Fermi-surface-related itinerant magnetism which is beyond the description of the Heisenberg model.

With the knowledge at ambient pressure, we now investigate the pressure effect. The total energy, geometry and Cr magnetic moment of the leading magnetic instabilities under different pressure are shown in TAB. I. Under pressure, the magnitude of magnetic moment on each Cr atom m_{Cr} are slightly reduced, but the total energy difference between the competing magnetic phases ΔE are significantly reduced. In particular, ΔE between the ground state and lowest energy competing phases of 2×2 , 4×2 , 4×1 and 8×1 is reduced to within a few meVs. We argue that the long range magnetic order would be suppressed at high pressure, if the quantum fluctuations are fully considered. Nevertheless, the magnetism remains important even at high pressure, as the phonon calcu-

lations indicate the structure instability is robust under pressure up to 30 GPa in NM state (FIG. 2b). Experimentally, however, the structural transition occurs at relatively low temperature ($\sim 55\text{K}$) at ambient pressure, and is quickly suppressed by applying external pressure at 5 GPa. Therefore, we conclude that the electronic correlations and magnetic fluctuations are crucial in the current system of interest, even at high pressure/temperatures that long range magnetic orderings are suppressed. Furthermore, the external pressure has nontrivial effect on the electronic structure as well (FIG. 3). Most remarkably, the vHS bonding state around K become dispersive along M-K at high pressures. Around 5 GPa, a Lifshitz transition occurs and the vHS bonding state crosses the Fermi level. Such metallization of bonding state may contribute to the superconductivity[55, 56].

In conclusion, we have performed systematic study of the electronic structure and magnetism of CsCr_3Sb_5 . The ground state of CsCr_3Sb_5 at the ambient pressure is found to be 4×2 collinear antiferromagnetic SDW-type order. Under high pressure, the energy differences between competing orders are significantly suppressed, suggesting enhanced magnetic frustration. Metallization of bonding state occurs around the critical pressure p_c , inducing a Lifshitz transition. These results supports an exotic ground state that enables spin-triplet pairing.

The authors are grateful to Xiaofeng Xu, Jinke Bao and Yi Liu for stimulating discussions. This work was support by NSFC (11874137, 12274364, 12304175), the National Key R&D Program of China (No. 2022YFA1402200), the Key R&D Program of Zhejiang Province (2021C01002), and the Zhejiang Provincial Natural Science Foundation of China (LQ23A040014). The calculations were performed on clusters at the High Performance Computing Cluster at Center of Correlated Matters Zhejiang University and High Performance Computing Center at Hangzhou Normal University.

* E-mail address: ccao@zju.edu.cn

† E-mail address: xiaoqunwang@zju.edu.cn

‡ E-mail address: hqlin@zju.edu.cn

- [1] J.-X. Yin, B. Lian, and M. Z. Hasan, *Nature* **612**, 647 (2022).
- [2] I. Syözi, *Progress of Theoretical Physics* **6**, 306 (1951), <https://academic.oup.com/ptp/article-pdf/6/3/306/5239621/273-B06SpdKu>.
- [3] S. Yan, D. A. Huse, and S. R. White, *Science* **332**, 1173 (2011).
- [4] L. Messio, B. Bernu, and C. Lhuillier, *Physical Review Letters* **108**, 207204 (2012).
- [5] S. Depenbrock, I. P. McCulloch, and U. Schollwöck, *Physical Review Letters* **109**, 067201 (2012).
- [6] Z. Y. Xie, J. Chen, J. F. Yu, X. Kong, B. Normand, and T. Xiang, *Physical Review X* **4**, 011025 (2014).
- [7] S.-S. Gong, W. Zhu, L. Balents, and D. N. Sheng, *Physical Review B* **91**, 075112 (2015).
- [8] S. Bieri, L. Messio, B. Bernu, and C. Lhuillier, *Physical Review B* **92**, 060407 (2015).
- [9] H. J. Liao, Z. Y. Xie, J. Chen, Z. Y. Liu, H. D. Xie, R. Z. Huang, B. Normand, and T. Xiang, *Physical Review Letters* **118**, 137202 (2017).
- [10] Y.-F. Jiang, H. Yao, and F. Yang, *Physical Review Letters* **127**, 187003 (2021).
- [11] Z. Cai, S. Chen, and Y. Wang, *Journal of Physics: Condensed Matter* **21**, 456009 (2009).
- [12] H. J. Changlani and A. M. Läuchli, *Physical Review B* **91**, 100407 (2015).
- [13] T. Liu, W. Li, A. Weichselbaum, J. von Delft, and G. Su, *Physical Review B* **91**, 060403 (2015).
- [14] E. Tang, J.-W. Mei, and X.-G. Wen, *Phys. Rev. Lett.* **106**, 236802 (2011).
- [15] Z. Lin, J.-H. Choi, Q. Zhang, W. Qin, S. Yi, P. Wang, L. Li, Y. Wang, H. Zhang, Z. Sun, L. Wei, S. Zhang, T. Guo, Q. Lu, J.-H. Cho, C. Zeng, and Z. Zhang, *Phys. Rev. Lett.* **121**, 096401 (2018).
- [16] F. Pollmann, P. Fulde, and K. Shtengel, *Physical Review Letters* **100**, 136404 (2008).
- [17] “Negative flat band magnetism in a spin-orbit-coupled correlated kagome magnet — Nature Physics,” <https://www.nature.com/articles/s41567-019-0426-7>.
- [18] W.-H. Ko, P. A. Lee, and X.-G. Wen, *Phys. Rev. B* **79**, 214502 (2009).
- [19] S.-L. Yu and J.-X. Li, *PHYSICAL REVIEW B* (2012).
- [20] M. L. Kiesel, C. Platt, and R. Thomale, *Phys. Rev. Lett.* **110**, 126405 (2013).
- [21] W.-S. Wang, Z.-Z. Li, Y.-Y. Xiang, and Q.-H. Wang, *PHYSICAL REVIEW B* (2013).
- [22] B. R. Ortiz, L. C. Gomes, J. R. Morey, M. Winiarski, M. Bordelon, J. S. Mangum, I. W. H. Oswald, J. A. Rodriguez-Rivera, J. R. Neilson, S. D. Wilson, E. Ertekin, T. M. McQueen, and E. S. Toberer, *Phys. Rev. Mater.* **3**, 094407 (2019).
- [23] B. R. Ortiz, S. M. L. Teicher, Y. Hu, J. L. Zuo, P. M. Sarte, E. C. Schueller, A. M. M. Abeykoon, M. J. Krogstad, S. Rosenkranz, R. Osborn, R. Seshadri, L. Balents, J. He, and S. D. Wilson, *Phys. Rev. Lett.* **125**, 247002 (2020).
- [24] H. Li, T. T. Zhang, T. Yilmaz, Y. Y. Pai, C. E. Marvinney, A. Said, Q. W. Yin, C. S. Gong, Z. J. Tu, E. Vescovo, C. S. Nelson, R. G. Moore, S. Murakami, H. C. Lei, H. N. Lee, B. J. Lawrie, and H. Miao, *Phys. Rev. X* **11**, 031050 (2021).
- [25] Z. Wang, Y.-X. Jiang, J.-X. Yin, Y. Li, G.-Y. Wang, H.-L. Huang, S. Shao, J. Liu, P. Zhu, N. Shumiya, M. S. Hossain, H. Liu, Y. Shi, J. Duan, X. Li, G. Chang, P. Dai, Z. Ye, G. Xu, Y. Wang, H. Zheng, J. Jia, M. Z. Hasan, and Y. Yao, *Phys. Rev. B* **104**, 075148 (2021).
- [26] M. M. Denner, R. Thomale, and T. Neupert, *Phys. Rev. Lett.* **127**, 217601 (2021).
- [27] H. Li, Y.-J. Yan, R. Yin, W. Xia, S. Fang, Z. Chen, Y. Li, W. Yang, Y. Guo, and D.-L. Feng, *Phys. Rev. Lett.* **127**, 187004 (2021).
- [28] H. Zhao, H. Li, B. R. Ortiz, S. M. L. Teicher, T. Park, M. Ye, Z. Wang, L. Balents, S. D. Wilson, and I. Zeljkovic, *Nature* **599**, 216 (2021).
- [29] H. Li, H. Zhao, B. R. Ortiz, T. Park, M. Ye, L. Balents, Z. Wang, S. D. Wilson, and I. Zeljkovic, *Nature Physics* **18**, 265 (2022).
- [30] H. Chen, H. Yang, B. Hu, Z. Zhao, J. Yuan, Y. Xing, G. Qian, Z. Huang, G. Li, Y. Ye, S. Ma, S. Ni, H. Zhang,

- Q. Yin, C. Gong, Z. Tu, H. Lei, H. Tan, S. Zhou, C. Shen, X. Dong, B. Yan, Z. Wang, and H.-J. Gao, *Nature* **599**, 222 (2021).
- [31] Z. Liu, N. Zhao, Q. Yin, C. Gong, Z. Tu, M. Li, W. Song, Z. Liu, D. Shen, Y. Huang, K. Liu, H. Lei, and S. Wang, *Phys. Rev. X* **11**, 041010 (2021).
- [32] M. Kang, S. Fang, J.-K. Kim, B. R. Ortiz, S. H. Ryu, J. Kim, J. Yoo, G. Sangiovanni, D. Di Sante, B.-G. Park, C. Jozwiak, A. Bostwick, E. Rotenberg, E. Kaxiras, S. D. Wilson, J.-H. Park, and R. Comin, *Nature Physics* **18**, 301 (2022).
- [33] Y.-X. Jiang, J.-X. Yin, M. M. Denner, N. Shumiya, B. R. Ortiz, G. Xu, Z. Guguchia, J. He, M. S. Hossain, X. Liu, J. Ruff, L. Kautzsch, S. S. Zhang, G. Chang, I. Belopolski, Q. Zhang, T. A. Cochran, D. Multer, M. Litskevich, Z.-J. Cheng, X. P. Yang, Z. Wang, R. Thomale, T. Neupert, S. D. Wilson, and M. Z. Hasan, *Nature Materials* **20**, 1353 (2021).
- [34] X. Feng, K. Jiang, Z. Wang, and J. Hu, *Science Bulletin* **66**, 1384 (2021).
- [35] L. Yu, C. Wang, Y. Zhang, M. Sander, S. Ni, Z. Lu, S. Ma, Z. Wang, Z. Zhao, H. Chen, K. Jiang, Y. Zhang, H. Yang, F. Zhou, X. Dong, S. L. Johnson, M. J. Graf, J. Hu, H.-J. Gao, and Z. Zhao, “Evidence of a hidden flux phase in the topological kagome metal csv_3sb_5 ,” (2021), arXiv:2107.10714 [cond-mat.supr-con].
- [36] N. Shumiya, M. S. Hossain, J.-X. Yin, Y.-X. Jiang, B. R. Ortiz, H. Liu, Y. Shi, Q. Yin, H. Lei, S. S. Zhang, G. Chang, Q. Zhang, T. A. Cochran, D. Multer, M. Litskevich, Z.-J. Cheng, X. P. Yang, Z. Guguchia, S. D. Wilson, and M. Z. Hasan, *Phys. Rev. B* **104**, 035131 (2021).
- [37] C. Mielke, D. Das, J. X. Yin, H. Liu, R. Gupta, Y. X. Jiang, M. Medarde, X. Wu, H. C. Lei, J. Chang, P. Dai, Q. Si, H. Miao, R. Thomale, T. Neupert, Y. Shi, R. Khasanov, M. Z. Hasan, H. Luetkens, and Z. Guguchia, *Nature* **602**, 245 (2022).
- [38] X. Wu, T. Schwemmer, T. Müller, A. Consiglio, G. Sangiovanni, D. Di Sante, Y. Iqbal, W. Hanke, A. P. Schnyder, M. M. Denner, M. H. Fischer, T. Neupert, and R. Thomale, *Phys. Rev. Lett.* **127**, 177001 (2021).
- [39] C. C. Zhao, L. S. Wang, W. Xia, Q. W. Yin, J. M. Ni, Y. Y. Huang, C. P. Tu, Z. C. Tao, Z. J. Tu, C. S. Gong, H. C. Lei, Y. F. Guo, X. F. Yang, and S. Y. Li, “Nodal superconductivity and superconducting domes in the topological kagome metal csv_3sb_5 ,” (2021), arXiv:2102.08356 [cond-mat.supr-con].
- [40] J. Zhao, W. Wu, Y. Wang, and S. A. Yang, *Phys. Rev. B* **103**, L241117 (2021).
- [41] W. Duan, Z. Nie, S. Luo, F. Yu, B. R. Ortiz, L. Yin, H. Su, F. Du, A. Wang, Y. Chen, X. Lu, J. Ying, S. D. Wilson, X. Chen, Y. Song, and H. Yuan, *Science China Physics, Mechanics & Astronomy* **64**, 107462 (2021).
- [42] C. Mu, Q. Yin, Z. Tu, C. Gong, H. Lei, Z. Li, and J. Luo, *Chinese Physics Letters* **38**, 077402 (2021).
- [43] C. Wang, J. Yu, Z. Zhang, and J.-H. Cho, “Phonon-mediated s-wave superconductivity in the kagome metal csv_3sb_5 under pressure,” (2023), arXiv:2303.10080 [cond-mat.supr-con].
- [44] Y. Zhong, S. Li, H. Liu, Y. Dong, K. Aido, Y. Arai, H. Li, W. Zhang, Y. Shi, Z. Wang, S. Shin, H. N. Lee, H. Miao, T. Kondo, and K. Okazaki, *Nature Communications* **14**, 1945 (2023).
- [45] F. Du, S. Luo, B. R. Ortiz, Y. Chen, W. Duan, D. Zhang, X. Lu, S. D. Wilson, Y. Song, and H. Yuan, *Phys. Rev. B* **103**, L220504 (2021).
- [46] C. C. Zhu, X. F. Yang, W. Xia, Q. W. Yin, L. S. Wang, C. C. Zhao, D. Z. Dai, C. P. Tu, B. Q. Song, Z. C. Tao, Z. J. Tu, C. S. Gong, H. C. Lei, Y. F. Guo, and S. Y. Li, *Phys. Rev. B* **105**, 094507 (2022).
- [47] E. M. Kenney, B. R. Ortiz, C. Wang, S. D. Wilson, and M. J. Graf, *Journal of Physics: Condensed Matter* **33**, 235801 (2021).
- [48] Y. Liu, Z.-Y. Liu, J.-K. Bao, P.-T. Yang, L.-W. Ji, J.-Y. Liu, C.-C. Xu, W.-Z. Yang, W.-L. Chai, J.-Y. Lu, C.-C. Liu, B.-S. Wang, H. Jiang, Q. Tao, Z. Ren, X.-F. Xu, C. Cao, Z.-A. Xu, J.-G. Cheng, and G.-H. Cao, “Superconductivity emerged from density-wave order in a kagome bad metal,” (2023), arXiv:2309.13514 [cond-mat.supr-con].
- [49] C. Cao, P. J. Hirschfeld, and H.-P. Cheng, *Phys. Rev. B* **77**, 220506 (2008).
- [50] D. J. Singh and M.-H. Du, *Phys. Rev. Lett.* **100**, 237003 (2008).
- [51] I. I. Mazin, M. D. Johannes, L. Boeri, K. Koepernik, and D. J. Singh, *Phys. Rev. B* **78**, 085104 (2008).
- [52] H. Jiang, G. Cao, and C. Cao, *Scientific Reports* **5**, 16054 (2015).
- [53] X.-X. Wu, C.-C. Le, J. Yuan, H. Fan, and J.-P. Hu, *Chinese Physics Letters* **32**, 057401 (2015).
- [54] L. Šmejkal, J. Sinova, and T. Jungwirth, *Phys. Rev. X* **12**, 040501 (2022).
- [55] M. Gao, X.-W. Yan, Z.-Y. Lu, and T. Xiang, *Phys. Rev. B* **104**, L100504 (2021).
- [56] H. Sun, M. Huo, X. Hu, J. Li, Z. Liu, Y. Han, L. Tang, Z. Mao, P. Yang, B. Wang, J. Cheng, D.-X. Yao, G.-M. Zhang, and M. Wang, *Nature* (2023), 10.1038/s41586-023-06408-7.